ON EXPLICIT LOWER BOUNDS AND BLOW-UP TIMES IN A MODEL OF CHEMOTAXIS

Maria Antonietta Farina

Department of Mathematics and Computer Science
University of Cagliari
V. Ospedale 72, 09124. Cagliari (Italy)

Monica Marras and Giuseppe Viglialoro

Department of Mathematics and Computer Science
University of Cagliari
V. le Merello 92, 09123. Cagliari (Italy)

Abstract. This paper is concerned with a parabolic Keller-Segel system in $\mathbb{R}^n$, with $n = 2$ or 3, under Neumann boundary conditions. First, important theoretical and general results dealing with lower bounds for blow-up time estimates are summarized and analyzed. Next, a resolution method is proposed and used to both compute the real blow-up times of such unbounded solutions and analyze and discuss some of their properties.

1. **Introduction.** In 1970 Keller and Segel proposed a mathematical model of chemotaxis phenomena; it consists of a system of parabolic equations (see [7]), whose solution describes the movement of cells in a bounded domain in response to the presence of a chemical substance which is inhomogeneously distributed in space. The mathematical formulation of this problem is prescribed by the following system of PDEs:

$$\begin{cases} u_t = \nabla \cdot (\mu \nabla u - \chi u \nabla v), \\ \tau v_t = \Delta v - k^2 v + u. \end{cases} \tag{1}$$

In system (1) the spatial distribution of the cells/bacteria is identified with the function u and that of the chemical substance/chemoattractant with v. The chemoattractant spreads diffusively and decays with rate k^2; it is also produced by the bacteria with rate 1. The bacteria diffuse with mobility μ and also drift in the direction of the gradient of the concentration of the chemoattractant with velocity $\chi |\nabla v|$; χ is called chemosensitivity. Furthermore, the parameter $\tau \geq 0$ is a measure of the ratio of the time scales of the cell movement and the distribution of the chemical. Once an initial distribution for both the bacteria and the chemical is given, the homogeneous Neumann boundary conditions represent the most natural and real situation of system (1); no net flux of the distributions with the external domain is permitted.

By rescaling the equations, we can always rewrite (1) with $\tau = 0$ or $\tau = 1$; in the former case the model is called parabolic-elliptic and in the latter parabolic-parabolic. In particular, for the parabolic-elliptic the spread rates degenerate to infinite, i.e. the chemical diffuses much faster than the cells move. We refer to paper [6] for a series of results dealing with some properties of the solutions of (1) in the parabolic-elliptic case.

In this manuscript we are interested in *chemotactic collapse*, a phenomenon connected to the same model (1); it is experimentally observed that the bacteria may concentrate in one or more points (see [5]). On the other hand, as discussed in [3] and [4], the so called isothermal collapse (related to relativistic or ultra-cold gases) represents another possible singular scenario.

From a mathematical point of view, the collapse corresponds to the blow-up of the solution at some finite time $t^\star$. In this sense, the blow-up phenomena of solutions to various problems, particularly for nonlinear parabolic systems, have received considerable attention (see, for instance, [9]-[14]).

Specifically, this work is concerned with the behavior of nonnegative and classical solutions $(u, v) = (u(\mathbf{x}, t), v(\mathbf{x}, t))$, with $\mathbf{x} = (x_1, \ldots, x_n)$ for $n = 2$ or 3, of the following system

$$\begin{cases} u_t = \Delta u - k_1 \nabla \cdot (u \nabla v), & \mathbf{x} \in \Omega, \ t \in (0, t^\star), \\ v_t = k_2 \Delta v - k_3 v + k_4 u, & \mathbf{x} \in \Omega, \ t \in (0, t^\star), \\ u_{\boldsymbol{\nu}} = 0 \ \text{and} \ v_{\boldsymbol{\nu}} = 0, & \mathbf{x} \in \partial \Omega, \ t \in (0, t^\star), \\ u = u_0(\mathbf{x}) \geq 0 \ \text{and} \ v = v_0(\mathbf{x}) \geq 0, & \mathbf{x} \in \Omega, \end{cases} \quad (2)$$

where Ω is a regular domain of $\mathbb{R}^n$, whose boundary $\partial \Omega$ is sufficiently smooth, $\boldsymbol{\nu} = (\nu_1, \ldots, \nu_n)$ stands for the unit outer normal to $\partial \Omega$, k_I ($I = 1, 2, 3, 4$) are positive constants, and $u_0(\mathbf{x})$ and $v_0(\mathbf{x})$ are nonnegative functions satisfying the corresponding compatibility conditions on $\partial \Omega$.

We focus our attention on lower bounds and blow-up times of unbounded solutions of problem (2). Precisely, in §2 we recall the main results obtained by Payne and Song in [15]; in this work the authors derive a first order time dependent differential inequality by means of an appropriate auxiliary function (herein called W-norm) of the solution of (2), depending on u and Δv. Subsequently, they give an explicit lower bound of $t^\star$ in the sense of this norm, for both $n = 2$ and $n = 3$, by means of analytical techniques. This lower bound estimate depends on the geometry of Ω, on the data k_I ($I = 1, 2, 3, 4$), and on $u_0(\mathbf{x})$ and $v_0(\mathbf{x})$.

Furthermore, there exist numerous papers devoted to the quantitative analysis of blowing up solutions of problems defined on bounded or unbounded domains (see for example [1] and [2]). In this sense, §3 deals with the resolution of problem (2); starting from its weak formulation, we propose an algorithm based on a mixed Finite Element Method in space and Euler Method in time (see [8]) capable of numerically solving the above system. This resolution approach is implemented in the 2D case to analyze the behaviors of the aforementioned W-norm as well of the infinity norm (indicated with L-norm) of some blowing up solutions of (2); more precisely, the values of the corresponding blow-up times in these two norms and evolutions of the blow-up spatial point are studied.

Finally, the paper is complemented by some conclusions (§4).

2. **An explicit lower bound: main results.** To derive a lower bound of the blow-up time $t^\star$ of a solution (u, v) of (2), let us introduce the auxiliary function

$$W(t) = \alpha \int_\Omega u^2 d\mathbf{x} + \int_\Omega (\Delta v)^2 d\mathbf{x}, \tag{3}$$

for some positive constant α to be specified, and also give the following

Definition 2.1. A classical solution (u, v) of (2) blows up in W-norm (3) at time $t^\star$ if

$$\lim_{t \to t^\star} W(t) = \infty.$$

As we said, the details of these two theorems are available in paper [15]; precisely, by using the same nomenclature we have:

Theorem 2.2. *(Lower bound for $t^\star$ in the 2D case; $n = 2$). Let (u, v) be a classical solution of (2), Ω being a bounded and convex domain in $\mathbb{R}^2$, with the origin inside. Assume $\alpha = \frac{k_4^2}{k_2}$. If (u, v) becomes unbounded in W-norm (3) at some finite time $t^\star$, then an estimate from below for $t^\star$ is given by*

$$t^\star \geq \int_{W_0}^\infty \frac{d\eta}{A_1 \eta^{\frac{3}{2}} + B_1 \eta^2}, \tag{4}$$

where $W_0 = W(0) = \alpha \int_\Omega u_0^2 d\mathbf{x} + \int_\Omega (\Delta v_0)^2 d\mathbf{x}$, A_1 and B_1 being positive constants depending on the geometry of Ω and on the constant k_I $(I = 1, 2, 3, 4)$.

Theorem 2.3. *(Lower bound for $t^\star$ in the 3D case; $n = 3$). Let (u, v) be a classical solution of (2), Ω being a bounded and convex domain in $\mathbb{R}^3$, with the origin inside. Assume $\alpha = \frac{k_4^2}{k_2}$. If (u, v) becomes unbounded in W-norm (3) at some finite time $t^\star$, then an estimate from below for $t^\star$ is given by*

$$t^\star \geq \int_{W_0}^\infty \frac{d\eta}{A\eta^{\frac{3}{2}} + B\eta^3}, \tag{5}$$

where $W_0 = W(0) = \alpha \int_\Omega u_0^2 d\mathbf{x} + \int_\Omega (\Delta v_0)^2 d\mathbf{x}$, A and B being positive constants depending on the geometry of Ω and on the constant k_I $(I = 1, 2, 3, 4)$.

Remark 1. By analyzing the proofs of Theorems 2.2 and 2.3, it is seen that since the constants A_1, B_1, A and B are not uniquely determined, neither estimate in (4) and in (5) is. In this sense they represent one of the possible lower bounds of $t^\star$ in the W-norm. On the other hand, the integrals in (4) and in (5) can be explicitly computed:

$$\int_{W_0}^\infty \frac{d\eta}{A_1 \eta^{\frac{3}{2}} + B_1 \eta^2} = \frac{2}{A_1 \sqrt{W_0}} + \frac{B_1}{A_1^2} \log\left(\frac{B_1^2 W_0}{(A_1 + B_1 \sqrt{W_0})^2}\right), \tag{6}$$

and

$$\int_{W_0}^\infty \frac{d\eta}{A\eta^{\frac{3}{2}} + B\eta^3} = \frac{\sqrt{3}\pi B^{\frac{1}{3}}}{A^{\frac{4}{3}}} - \frac{2\sqrt{3}B^{\frac{1}{3}}}{3A^{\frac{4}{3}}} \arctan\left(\frac{A^{\frac{1}{3}} - 2B^{\frac{1}{3}}\sqrt{W_0}}{\sqrt{3}A^{\frac{1}{3}}}\right)$$
$$+ \frac{2}{A\sqrt{W_0}} + \frac{B^{\frac{1}{3}}}{3A^{\frac{4}{3}}} \log\left(\frac{A^{\frac{2}{3}} - A^{\frac{1}{3}}B^{\frac{1}{3}}\sqrt{W_0} + B^{\frac{2}{3}}W_0}{(A^{\frac{1}{3}} + B^{\frac{1}{3}}\sqrt{W_0})^2}\right). \tag{7}$$

First of all, let us underline that the expression $A^{\frac{2}{3}} - A^{\frac{1}{3}}B^{\frac{1}{3}}\sqrt{W_0} + B^{\frac{2}{3}}W_0$ is positive, so that the logarithm in (7) is well defined. Moreover, (6) and (7) decrease with W_0 increasing (actually also $t^\star$ does, as shown in examples of §3.2.1); as a consequence, if W_0 is large enough, both estimates are very close to zero. Therefore, since the

existence of blowing up solutions of (2) is also linked to the magnitudes of its initial data (i.e., W_0), we expect that the real value of $t^\star$ is in general considerably larger than the estimates given in the two theorems (see some examples in [16]).

We conclude this section by mentioning that in [13] the authors of this manuscript investigate system (2) under a more general assumption, consisting of choosing $k_I = k_I(t)$ ($I = 1, 2, 3, 4$) and non constant; in fact, the time dependence of these coefficients may affect the behavior of the solution (u, v).
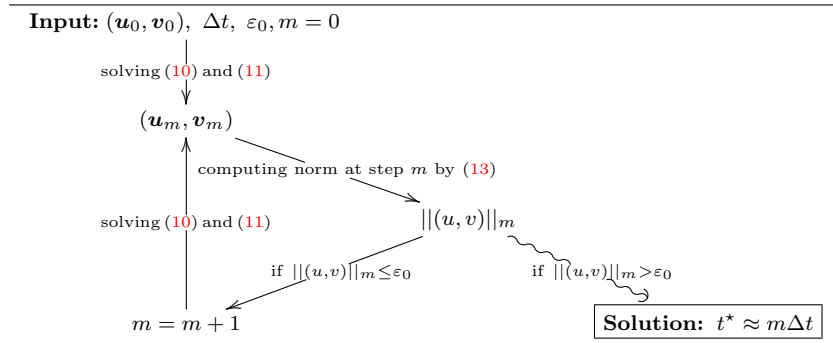
Input: $(\boldsymbol{u}_0, \boldsymbol{v}_0)$, Δt, $\varepsilon_0, m = 0$

solving (10) and (11)

$(\boldsymbol{u}_m, \boldsymbol{v}_m)$

computing norm at step m by (13)

solving (10) and (11) $||(u, v)||_m$

if $||(u,v)||_m \leq \varepsilon_0$ if $||(u,v)||_m > \varepsilon_0$

$m = m + 1$ **Solution:** $t^\star \approx m\Delta t$

TABLE 1. Computation of the blow-up time $t^\star$. The necessary input data are the threshold ε_0, the time step Δt and the initial datum $(\boldsymbol{u}_0, \boldsymbol{v}_0)$; subsequently, it is possible to calculate the sequences $(\boldsymbol{u}_m, \boldsymbol{v}_m)$ and $||(u, v)||_m$ and, consequently, to compute $t^\star$. Let us clarify that if $||(u, v)||_m = W_m$ (respectively, L_m) $t^\star$ represents $t^\star_W$ (respectively, $t^\star_L$)

3. **Numerical resolution method.** Let us give a resolution method for system (2). We propose a mixed Finite Element Method in space and Euler Method in time algorithm. Let us point out that even though Euler's approximation produces results with first order precision, it is totally appropriate to the aims of our research (see [16]).

3.1. **Finite element method: semi-discretization in space.** If a mesh of $\Omega \subset \mathbb{R}^n$ ($n = 2$ and 3) is fixed and N represents the total number of nodes of Ω, let $(\mathcal{U}, \mathcal{V})$ be the numerical approximation of the solution (u, v) of (2): therefore, by separating variables

$$\begin{cases} \mathcal{U}(\mathbf{x}, t) = \sum_{i=1}^N u^i(t)\varphi^i(\mathbf{x}), \\ \mathcal{V}(\mathbf{x}, t) = \sum_{i=1}^N v^i(t)\varphi^i(\mathbf{x}), \end{cases} \tag{8}$$

where $\varphi^i(\mathbf{x})$ is the standard quadratic basis function at the vertex $\mathbf{x}^i$, for $i = 1, ..., N$. Thanks to the divergence theorem and the homogeneous boundary conditions of system (2), by multiplying its first two equations by a generic test function $\varphi^j(\mathbf{x})$, the following variational form in space is achieved:

$$\begin{cases} (\mathcal{U}_t, \varphi^j) + (\nabla\mathcal{U}, \nabla\varphi^j) = k_1(\mathcal{U}\nabla\mathcal{V}, \nabla\varphi^j), \\ (\mathcal{V}_t, \varphi^j) + k_2(\nabla\mathcal{V}, \nabla\varphi^j) = k_4(\mathcal{U}, \varphi^j) - k_3(\mathcal{V}, \varphi^j), \end{cases} \quad j = 1, \ldots, N, \, t \geq 0, \tag{9}$$

where $(\cdot, \cdot)$ denotes the usual L^2 inner product.

To compute the time evolutions of both coefficients u^i and v^i appearing in (8), let $\Delta t = t_{m+1} - t_m$ be a given time step, with $m = 0, 1, 2, \ldots$ ($t_0 = 0$), and $(\mathcal{U}_m, \mathcal{V}_m)$ the approximation of $(\mathcal{U}(\mathbf{x}, t), \mathcal{V}(\mathbf{x}, t))$ at time t_m. By applying an implicit Euler finite difference approximation to system (9), it is seen that

$$\begin{cases} (\frac{\mathcal{U}_{m+1} - \mathcal{U}_m}{\Delta t}, \varphi^j) + (\nabla \mathcal{U}_{m+1}, \nabla \varphi^j) = k_1 (\mathcal{U}_m \nabla \mathcal{V}_m, \nabla \varphi^j), \\ (\frac{\mathcal{V}_{m+1} - \mathcal{V}_m}{\Delta t}, \varphi^j) + k_2 (\nabla \mathcal{V}_{m+1}, \nabla \varphi^j) = k_4 (\mathcal{U}_m, \varphi^j) - k_3 (\mathcal{V}_m, \varphi^j), \end{cases}$$

i.e., taking into account (8),

$$\boldsymbol{M} \frac{\boldsymbol{u}_{m+1} - \boldsymbol{u}_m}{\Delta t} + \boldsymbol{K} \boldsymbol{u}_{m+1} = k_1 \mathcal{F}(\boldsymbol{u}_m, \boldsymbol{v}_m), \tag{10}$$

and

$$\boldsymbol{M} \frac{\boldsymbol{v}_{m+1} - \boldsymbol{v}_m}{\Delta t} + k_2 \boldsymbol{K} \boldsymbol{v}_{m+1} = k_4 \boldsymbol{M} \boldsymbol{u}_m - k_3 \boldsymbol{M} \boldsymbol{v}_m, \tag{11}$$

with $\boldsymbol{M} \in \mathbb{R}^{N \times N}$ (mass matrix), $\boldsymbol{K} \in \mathbb{R}^{N \times N}$ (stiffness matrix) and $\mathcal{F}(\boldsymbol{u}_m, \boldsymbol{v}_m) \in \mathbb{R}^N$ such that

$$\begin{cases} M_{ij} = \int_\Omega \varphi^i(\mathbf{x}) \varphi^j(\mathbf{x}) d\mathbf{x}, \\ K_{ij} = \int_\Omega \nabla \varphi^i(\mathbf{x}) \cdot \nabla \varphi^j(\mathbf{x}) d\mathbf{x}, \\ \mathcal{F}(\boldsymbol{u}_m, \boldsymbol{v}_m)_j = \int_\Omega (\sum_{p,q=1}^N u_m^p v_m^q \varphi^p(\mathbf{x}) \nabla \varphi^q(\mathbf{x})) \cdot \nabla \varphi^j(\mathbf{x}) d\mathbf{x}, \end{cases}$$

being $\boldsymbol{u}_m = (u_m^1, \ldots, u_m^N)^T$ and $\boldsymbol{v}_m = (v_m^1, \ldots, v_m^N)^T$, where T indicates the transposition operator. Under these circumstances, (u_m^i, v_m^i) represents the approximation of the solution (u, v) of problem (2) at time t_m, for $m = 0, 1, 2, \ldots$, and at space point $\mathbf{x}^i$, for $i = 1, 2, \ldots, N$.

In this way the *continuous* solution of the *nonlinear* system (2) is identified to the *discrete* solution of the *linear* system composed by (10) and (11)

3.2. **Numerical algorithm: computing the blow-up times.** Theorems 2.2 and 2.3 return an estimate of a lower bound for the blow-up time of positive solutions of (2) in terms of W-norm (3). In this section we will analyze the blow-up phenomena also by considering the natural infinity norm (indicated with L-norm) of a solution (u, v) of the same system (see [5]):

$$L(t) = \max \left\{ \max_{\mathbf{x} \in \overline{\Omega}} |u(\mathbf{x}, t)|, \max_{\mathbf{x} \in \overline{\Omega}} |v(\mathbf{x}, t)| \right\}. \tag{12}$$

Definition 3.1. A classical solution (u, v) of (2) blows up in L-norm (12) at time $t^\star$ if

$$\lim_{t \to t^\star} L(t) = \infty.$$

By means of the numerical approach presented in §3.1, we want to compare the blow-up times in the sense of the W-norm and the L-norm. We indicate these values with $t_W^\star$ and $t_L^\star$; of course, they depend on the temporal evolutions of the W and L norms, respectively.

To this end, first of all, we need to numerically quantify the values of the W-norm and the L-norm at step m, i.e. $W_m = W(t_m)$ and $L_m = L(t_m)$; according to (3) and (12), we can define

$$\begin{cases} W_m = \alpha \int_\Omega \left(\sum_{i=1}^n u_m^i \varphi^i(\mathbf{x}) \right)^2 d\mathbf{x} + \int_\Omega \left(\sum_{i=1}^n v_m^i \Delta \varphi^i(\mathbf{x}) \right)^2 d\mathbf{x}, \\ L_m = \max \left\{ \max_{i=1,\ldots,N} |u_m^i|, \max_{i=1,\ldots,N} |v_m^i| \right\}, \end{cases} \tag{13}$$

with α as in Theorems 2.2 and 2.3. Therefore, we propose the following algorithm to calculate $t_W^\star$ (i.e. $t_L^\star$) for unbounded solutions of (2). Let ε_0 be a fixed threshold: once the initial data $(\boldsymbol{u}_0, \boldsymbol{v}_0)$ is given, $\boldsymbol{u}_1$ and $\boldsymbol{v}_1$ are computed from (10) and (11), respectively. Subsequently, $(\boldsymbol{u}_1, \boldsymbol{v}_1)$ is used to update $(\boldsymbol{u}_2, \boldsymbol{v}_2)$, and so on; we exit the loop when the W-norm (i.e. the L-norm) of the solution at step m, W_m (i.e. L_m), is larger than the initial threshold ε_0 (*Stopping Criterion*); consequently, $t_W^\star \approx m\Delta t$ (i.e. $t_L^\star \approx m\Delta t$). The scheme in Table 1 summarizes this algorithm.

3.2.1. *Numerical tests for $n = 2$.* Let us consider the domain $Q = \Omega \times \mathbb{R}_0^+$, being $\Omega = [-2, 2] \times [-2, 2]$ the square with center in the origin of the axes $O = (0, 0)$ and length 4. We take a uniform mesh, obtained by dividing each side of the square into 200 equal parts (i.e. 40401 vertexes and 80000 triangles). We also choose $v_0(\mathbf{x}) = 0.55 e^{-(x^2+y^2)}(4 - x^2)^2(4 - y^2)^2$ as initial condition (the chemical signal at time $t_0 = 0$), and $\varepsilon_0 = 10^6$ as the threshold and $\Delta t = 10^{-4}$ as the integration step. Moreover, we fix the following values for k_I: $k_1 = 0.2$, $k_2 = k_4 = 1$ and $k_3 = 0.1$. Once these data are set, we solve (2) in two cases, depending on the choice of the other initial condition $u_0(\mathbf{x})$ (the bacteria at time $t_0 = 0$):

Test 1: $u_0(\mathbf{x}) = 1.15 e^{-(x^2+y^2)}(4 - x^2)^2(4 - y^2)^2$;
Test 2: $u_0(\mathbf{x}) = 24(((x^2 - 4)^2 + (y^2 - 4)^2 + 1) - 0.05((x^2 - 4)^4 + (y^2 - 4)^4))$.

(a) Evolution of $\max_{\mathbf{x} \in \Omega} |u(\mathbf{x}, t)|$

(b) Evolution of $\max_{\mathbf{x} \in \Omega} |v(\mathbf{x}, t)|$

(c) Comparison between $\max_{\mathbf{x} \in \Omega} |u(\mathbf{x}, t)|$ (continuous line) and $\max_{\mathbf{x} \in \Omega} |v(\mathbf{x}, t)|$ (dashed line)

(d) Evolutions of $\alpha \int_\Omega u^2 d\mathbf{x}$ (continuous line) and $\int_\Omega (\Delta v)^2 d\mathbf{x}$ (dashed line)

(e) Comparison between the W-norm (continuous line) and the L-norm (dashed line)
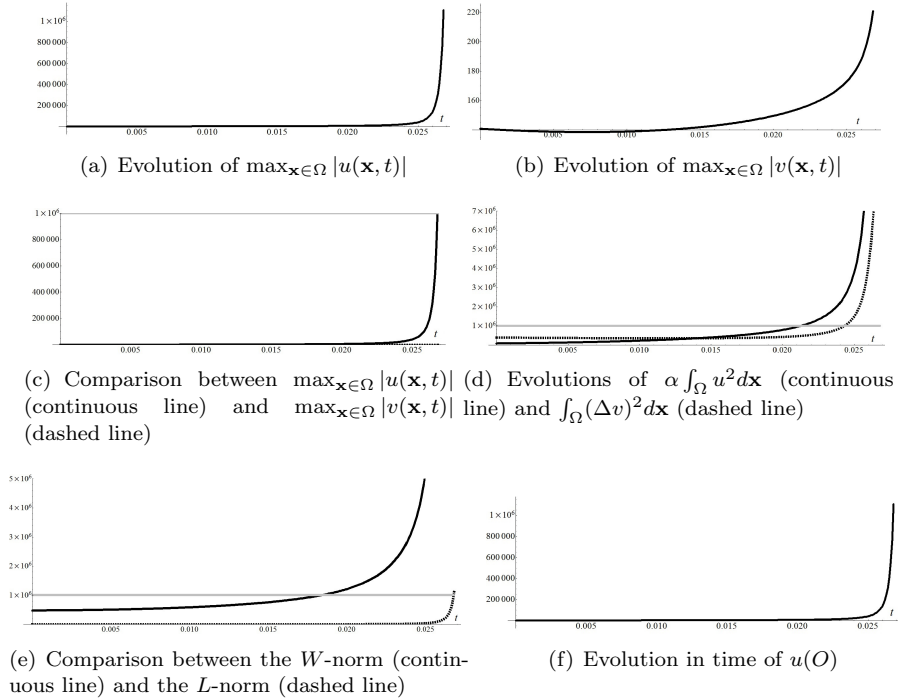
(f) Evolution in time of $u(O)$

FIGURE 1. Analysis of the behaviors of the W-norm and the L-norm in time; the horizontal clear line represents the threshold

We observe that both $v_0(\mathbf{x})$ and $u_0(\mathbf{x})$ chosen in tests 1 and 2 verify the compatibility conditions associated to system (2). The results obtained by running the algorithm

of §3.2 are presented in Table 2; it points out that the blow-up time in the sense of Definition 2.1 is smaller than the value computed in the sense of Definition 3.1. This is justified by the different behaviors of the two norms, W and L; in fact, Figures 1(e) and 3(a) show that the W-norm grows considerably faster with respect the L-norm. In the same table we can observe that the blow-up time decreases with increasing the corresponding norm of the initial data (see Remark 1). Furthermore, as we briefly discussed in §1, if the initial cell density is sufficiently large the phenomenon of cell aggregation is produced; the nonlocal chemical interaction dominates diffusion and results in a blow-up of the bacteria distribution, represented by function u. Both examples we are proposing obey this phenomenon; in either case, the contribution of the part of both norms W and L corresponding to u dominates that of v. In particular, for Test 1, this is observed in Figures 1(a), 1(b), 1(c) and 1(d).

(a) Solution u at time $t = 0.002$; $u(O) \approx 299.268$

(b) Solution u at time $t = 0.0067$; $u(O) \approx 796.96$

(c) Solution u at time $t = 0.0133$; $u(O) \approx 1874.53$

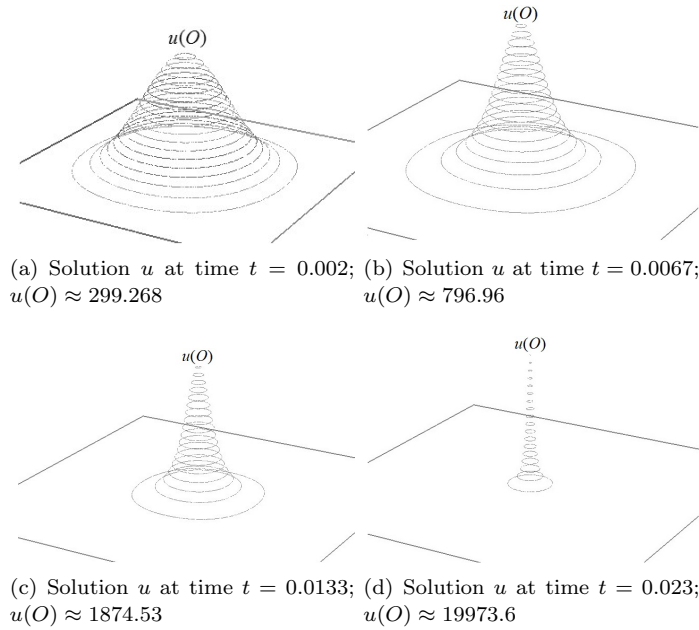(d) Solution u at time $t = 0.023$; $u(O) \approx 19973.6$

FIGURE 2. Test 1: numerical solution. Evolution of u and its graphical representation: with t increasing the value of u at O increases

On the other hand, let us also specify that the initial function u_0 of Test 1 has one peak in the origin O. The effect of the blow-up is to produce a larger and sharper peak at this same point (see Figure 2); Figure 1(f) exhibits the temporal evolution of $u(O)$, that in this case coincides with that of the L-norm. On the contrary, the initial function u_0 of Test 2 has four peaks in the points $P_1 = (x_0, y_0), P_2 = (x_0, -y_0), P_3 = (-x_0, y_0)$ and $P_4 = (-x_0, -y_0)$ (with $x_0 = y_0 = \sqrt{4 - \sqrt{10}}$), where it achieves the same value. As shown in Figure 4 they coalesce and produce a single peak in the origin O. More exactly, the values of u in these four points decrease while its value at the origin O, which initially represents a local minimum of u_0, increases and eventually blows up (Figures 3(b), 3(c) and 3(d)).

(a) Comparison between the W-norm (continuous line) and the L-norm (dashed line)

(b) Evolution of $u(P_1)$; $u(P_1), u(P_2), u(P_3)$ and $u(P_4)$ decrease

(c) Evolution in time of $u(O)$

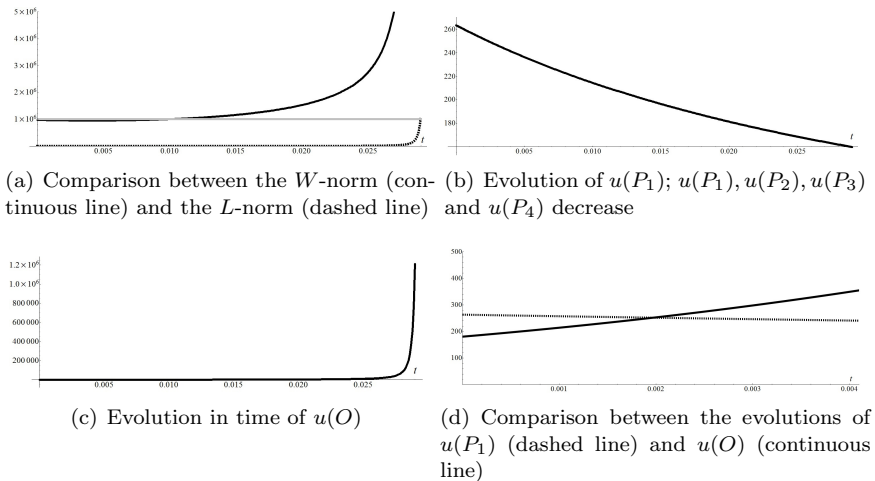(d) Comparison between the evolutions of $u(P_1)$ (dashed line) and $u(O)$ (continuous line)

FIGURE 3. Analysis of the behaviors of the W-norm and the L-norm in time; the horizontal clear line represents the threshold. Let us observe that value of u at the blow-up point O increases and absorbs $u(P_1), u(P_2), u(P_3)$ and $u(P_4)$; moreover, the evolution of u at these point is the same

	L_0	W_0	$t_L^\star$	$t_W^\star$
Test 1	299.26	481225	0.0268	0.0186
Test 2	263.39	975613	0.0291	0.0097

TABLE 2. Computing the blow-up times in the sense of the W-norm and the L-norm

Remark 2. In another example we have chosen as initial data a compatible function $u_0(\mathbf{x})$ presenting four peaks, none at the origin O and one of them considerably larger than the other peaks and situated at the point $(-1, -1)$ of $[-2, 2] \times [-2, 2]$; also in this case the values at these points decrease contrary to that at the origin which increases; finally, they coalesce and produce a single peak in O.

4. **Conclusions.** In this work we have discussed some aspects of a two and three dimensional Keller-Segel system connected to chemotaxis phenomena. Specifically, the blowing up behaviors of its positive solutions have been analyzed. We have started by reviewing theoretical results concerning lower bounds of unbounded solutions in terms of an appropriate norm (the W-norm). In parallel, we have also proposed a numerical resolution algorithm for the same system; it consists of a mixed finite-difference and finite-element method. We have applied this algorithm and given some numerical results for the 2D case; it is shown that with a fixed integration step highly concentrated blowing up solutions can be successfully captured. In this sense, we have computed the blow-up time $t_W^\star$ in terms of the W-norm and also $t_L^\star$, i.e. that obtained in terms of the more natural infinity norm (the L-norm). Moreover, an analysis of the temporal evolution of these norms has been carried out; we observe that even though the W-norm increases considerably faster with respect to the L-norm, $t_W^\star$ is not so much smaller than $t_L^\star$. Moreover, the analysis

(a) Solution u at time $t = 0.001$; $u(O) \approx 263.38$

(b) Solution u at time $t = 0.007$; $u(O) \approx 540.75$

(c) Solution u at time $t = 0.013$; $u(O) \approx 1223.53$

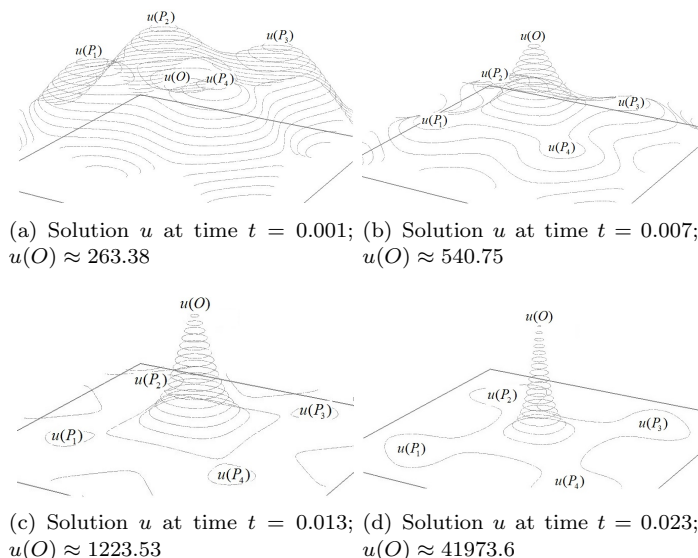(d) Solution u at time $t = 0.023$; $u(O) \approx 41973.6$

FIGURE 4. Test 2: numerical solution. Evolution of u and its graphical representation: with t increasing the value of u in O increases and the values of u in P_1, P_2, P_3 and P_4 decrease, even with the same behaviors

of the proposed tests also allows us to conclude that the method is coherent with the expected results: in fact, for instance, the solution depends on that of the corresponding initial function and the more the initial norm (as much W as well L) increases the more the associated blow-up time decreases.

REFERENCES

[1] G. Acosta, R. G: Duran and J.D. Rossi, An adaptive time step procedure for a parabolic problem with blow-up, *Computing.*, **68** (2002), 343–373

[2] C. Bandle and H. Brunner, Blowup in diffusion equations: A survey, *J. Comput. Appl. Math.*, **97** (1998), 3–22

[3] M.C. Carrisi, A further condition in the extended macroscopic approach to relativistic gases, *Int. J. Pure Appl. Math.*, **67** (2011), 259–289

[4] M.C. Carrisi and S. Mignemi, Snyder-de Sitter model from two-time physics, *Phys. Rev. D.*, **82**, no. 105031 (2010), 5 pages

[5] D. Horstmann, From 1970 until present: The Keller-Segel model in chemotaxis and its consequences, *I. Jahresber. Deutsche Math. Verein.*, **105** (2003), 103–165

[6] W. Jäger and S. Luckhaus, On explosions of solutions to a system of partial differential equations modelling chemotaxis, *Trans. Amer. Math. Soc.*, **329** (1992), 819–824

[7] E. F. Keller and A. Segel, Initiation of slime mold aggregation viewed as an instability, *J. Theoret. Biol.*, **26** (1970), 399–415

[8] S. Larsson and V. Thomée, *Partial Differential Equations with Numerical Methods*, Springer-Verlag, 2003

[9] M. Marras, Bounds for blow-up time in nonlinear parabolic systems under various boundary conditions, *Num. Funct. Anal. Optim.*, **32** (2011), 453– 468

[10] M. Marras and S. Vernier Piro, Bounds for blow-up time in nonlinear parabolic systems, *Discret. Contin. Dyn. Syst., Suppl.*, (2011), 1025–1031

[11] M. Marras and S. Vernier Piro, Blow-up phenomena in reaction-diffusion systems, *Discret. Contin. Dyn. Syst.*, **32** (2012), 4001–4014

[12] M. Marras, S. Vernier-Piro and G. Viglialoro, Estimate from below of blow-up time in a parabolic system with gradient term, *Int. J. Pure Appl. Math.*, **93** (2014), 297–306

[13] M. Marras, S. Vernier-Piro and G. Viglialoro, Lower bounds for blow-up in a parabolic-parabolic Keller-Segel system, *Submitted*

[14] L. E. Payne and G. A. Philippin, Blow-up Phenomena for a Class of Parabolic Systems with Time Dependent Coefficients, *Appl. Math.*, **3** (2012), 325–330

[15] L. E. Payne and J.C. Song, Lower bound for blow-up in a model of chemotaxis, *J. Math. Anal. Appl.*, **385** (2012), 672–676

[16] G. Viglialoro, On the blow-up time of a parabolic system with damping terms, *C. R. Math.*, **67** (2014), 1223–1232

Received xxxx 20xx; revised xxxx 20xx.

E-mail address: mafarina@unica.it
E-mail address: mmarras@unica.it
E-mail address: giuseppe.viglialoro@unica.it